2014

Condensation and Evaporation of R744/R32/R1234ze(E) Flow in Horizontal Microfin Tubes

Chieko Kondou
Kyushu University, Japan, kondo.chieko.162@m.kyushu-u.ac.jp

Fumiya Mishima
Kyushu University, Japan, mishima@phase.cm.kyushu-u.ac.jp

JinFan Liu
Kyushu University, Japan, liu@phase.cm.kyushu-u.ac.jp

Shigeru Koyama
Kyushu University, Japan, koyama@cm.kyushu-u.ac.jp

Condensation and Evaporation of R744/R32/R1234ze(E) Flow in Horizontal Microfin Tubes

Chieko KONDOU[1]*, Fumiya MISHIMA[1], JinFan LIU[1], Shigeru KOYAMA[1, 2]

[1] Kyushu University, Interdisciplinary Graduate School of Engineering Science, Fukuoka, Japan
*E-mail; kondo.chieko.162@m.kyushu-u.ac.jp

[2] Kyushu University, International Institute for Carbon-Neutral Energy Research, Fukuoka, Japan
E-mail; koyama@phase.cm.kyushu-u.ac.jp

ABSTRACT

The heat transfer characteristics of a low global warming potential (GWP) refrigerant mixture R744/R32/R1234ze(E) in a horizontal microfin tube were investigated in this study. The condensation heat transfer coefficient of R744 /R32/R1234ze(E) (9/29/62 mass%) is somewhat lower than that of other mixtures R744/R32/R1234ze(E) (4/43/53 mass%), R32/R1234ze(E) (40/60 mass%), and (30/70 mass%) at an average saturation temperature of 40 °C, mass flux of 200 kg $m^{-2}s^{-1}$, and heat flux of 10 kWm^{-2}. The temperature glides of R744/R32/R1234ze(E) (9/29/62 mass%), (4/43/53 mass%), R32/R1234ze(E) (30/70 mass%), and (40/60 mass%) are 18, 11, 10, and 8 K, respectively, at 40 °C. Likewise, the magnitude of the heat transfer coefficient decrease strongly affected the temperature glide. The data for the evaporation heat transfer coefficient indicated similar effects on the temperature glide. At an average saturation temperature of 10 °C, the evaporation heat transfer coefficient of R744/R32/R1234ze(E) (9/29/62 mass%) is slightly lower than that of other mixtures. The temperature glides of R744/R32/R1234ze(E) (9/29/62 mass%), (4/43/53 mass%), R32/R1234ze(E) (30/70 mass%), and (40/60 mass%) are 22, 13, 11, and 9 K, respectively. The pressure gradients of these refrigerants are almost equal, and the difference is within the measurement uncertainty. The experimental pressure gradient agrees well with the predictions proposed for single components.

1. INTRODUCTION

Low global warming potential (GWP) refrigerant R1234ze(E) has been considered as an alternative to conventional refrigerant R410A for air conditioning systems. However, the latest studies revealed that the coefficient of performance (COP) of systems using R1234ze(E) alone is unexpectedly lower than that of R410A. Because the volumetric capacity is much smaller than that of R410A, the cycle using R1234ze(E) requires a much higher volumetric flow rate with a larger compressor displacement or higher compressor speed to maintain the cooling/heating load, which results in a large pressure drop. The mixing of R744, R32, and R1234ze(E) has been recently attempted to increase the volumetric capacity while maintaining the global warming potential (GWP) below 300 (Koyama et al., 2013). The COP of the cycle using these ternary refrigerants has already been evaluated, and the feasibility was demonstrated with a drop-in experiment (Fukuda et al., 2014). Nevertheless, the characteristics of the heat transfer and pressure drop of these refrigerants have not yet been clarified. As mentioned in many previous studies (e.g., Jacobs and Kruse, 1978; McLinden and Radermacher, 1987), exergy loss in heat exchangers can be minimized by utilizing the temperature glide of zeotropic mixtures. However, volatility differences result in severe degradation of the heat transfer coefficient (HTC), as investigated in numerous heat transfer studies (e.g., Jung and Radermacher, 1993; Niederküger and Steiner, 1994).

To understand the transport phenomenon of these ternary mixtures, the HTC and pressure gradient during the condensation and evaporation process in a horizontal microfin tube was experimentally investigated in this study. Experimental data of R744/R32/R1234ze(E) (4/43/53 mass%) were compared to R32/R1234ze(E) (40/60 mass%) as the combination of GWP 300; data on R744/R32/R1234ze(E) (9/29/62 mass%) were compared to R32/R1234ze(E) (30/70 mass %) as the combination of GWP 200.

2. EXPERIMENTAL METHOD

Figure 1 (a) illustrates a vapor compression cycle that facilitated the measurement of the HTC and pressure gradient. The HTC and pressure gradient were measured in test sections (4) and (10) for condensation and evaporation, respectively. To determine the bulk enthalpies of superheated vapor, the bulk mean temperature and the pressure were measured in mixing chambers placed at the inlet of the desuperheater (3) and the outlet of the superheater (11). Additionally, the circulation composition of the mixture was measured by sampling approximately 1 cc of subcooled liquid at the outlet of the liquid reservoir (6) just after the data were recorded. The sampled liquid was completely vaporized in the sampling vessel and then assayed by a thermal conductivity detector gas chromatograph. The refrigerant state was always evaluated at the circulation composition. Based on the bulk enthalpies of the superheated vapor, the enthalpies in the test sections were calculated by considering the enthalpy changes in the desuperheater and superheater obtained from the water side heat balance.

Figure 1 (b) illustrates the structure of the test section (10) for the evaporation test. The structure of the other test section (4) for the condensation test was almost the same. A horizontally placed test microfin tube was surrounded by four water jackets and bored 0.6 mm ID pressure ports between the test sections to measure the heat transfer rates over the 414 mm length and pressure drops at 554 mm intervals. At the center of each subsection (i.e. the water jacket), four thermocouples were embedded in the outside tube wall. The internal tube surface temperature, T_{wi}, was obtained from the one-dimensional heat conduction in the tube wall.

$$T_{wi} = \left(T_{wo,top} + T_{wo,bottom} + T_{wo,right} + T_{wo,left}\right)/4 - \left[Q_{H2O\,TS}/\left(2\pi\Delta Z\,\lambda_{tube}\right)\right]\ln\left(D_o/d_{eq}\right) \quad (1)$$

The representative refrigerant temperature of each subsection, $T_{r\,TS}$, was defined as the arithmetic mean of the inlet and outlet calculated from the enthalpies and pressures by assuming thermodynamic equilibrium.

$$T_{r\,TS} = \left(T_{r\,TS,i} + T_{r\,TS,o}\right)/2 \quad (2)$$

$$T_{r\,TS,i} = f_{equilibrium}\left(h_{r\,TS,i}, P_{r\,TS,i}, X_{R744}, X_{R32}\right),\ T_{r\,TS,o} = f_{equilibrium}\left(h_{r\,TS,o}, P_{r\,TS,o}, X_{R744}, X_{R32}\right) \quad (3,\ 4)$$

Similarly, the representative vapor quality of each subsection, x, was calculated as follows:

$$x_{TS} = \left(x_{TS,i} + x_{TS,o}\right)/2 \quad (5)$$

$$x_{TS,i} = f_{equilibrium}\left(h_{r\,TS,i}, P_{r\,TS,i}, X_{R744}, X_{R32}\right),\ x_{TS,o} = f_{equilibrium}\left(h_{r\,TS,o}, P_{r\,TS,o}, X_{R744}, X_{R32}\right) \quad (6,\ 7)$$

Table 1 specifies the dimensions of the test microfin tube based on the symbols in the microscopic cross sectional

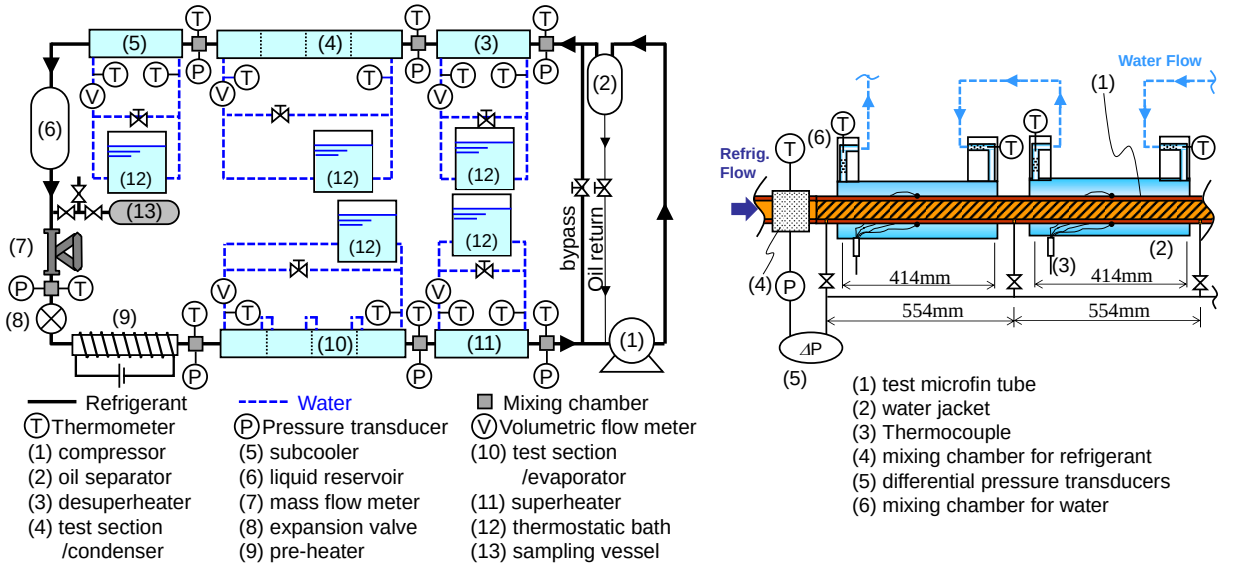

(a) diagram of the test loop (b) structure of the test section (for evaporation test)

Figure 1: Experimental apparatus

Table 1: Dimensions of test microfin tube

Outer diameter	D_o	6.0	mm
Fin root inner diameter	d_{max}	5.45	mm
Equivalent inner diameter	d_{eq}	5.35	mm
Fin height	h_{fin}	0.255	mm
Helix angle	β	20	deg.
Number of fins	N_{fin}	48	-
Surface enlargement	η_A	2.24	-

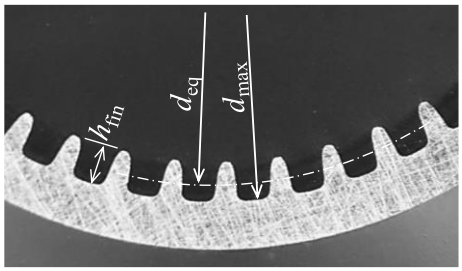

Figure 2: Microscopic cross section of the tube

Table 2: Comparison on thermophysical properties for the test refrigerants at equilibrium conditions

Refrigerant composition		R32/1234ze(E) (30/70 mass%)	R32/1234ze(E) (40/60 mass%)	R744/32/1234ze(E) (9/29/62 mass%)	R744/32/1234ze(E) (4/43/53 mass%)
GWP_{100}*[a]		207	274	200	293
at 40 °C*[b]	Pressure [MPa]	1.44	1.62	1.94	1.90
	Temperature glide [K]	10.3	9.0	18.7	11.8
	Latent heat of vaporization [kJ kg^{-1}]	187	194	199	201
	Density [kg m^{-3}] *[c]	1056/59	1031/62.4	1042/73.7	1015/69.8
	Viscosity [μPa s] *[c]	136/13.9	127/14.1	131/14.8	122/14.4
	Thermal conductivity [mW m^{-1} K^{-1}] *[c]	86.6/16.3	91.4/16.5	91.2/18.0	94.7/17.4
at 10 °C*[b]	Pressure [MPa]	0.62	0.70	0.87	0.84
	Temperature glide [K]	11.7	10.2	21.6	13.7
	Latent heat of vaporization [kJ kg^{-1}]	220	230	238	241
	Density [kg m^{-3}] *[c]	1168/24.9	1146/26.3	1161/32	1134/29.8
	Viscosity [μPa s] *[c]	194/12.5	180/12.6	191/13.1	175/12.8
	Thermal conductivity [mW m^{-1} K^{-1}] *[c]	101.4/13	107.4/13	108.4/14.2	112.2/13.4

*[a] GWPs of mixtures are simply weighed by the mass fraction. *[b] Average of dew and bubble temperatures.
*[c] These data at the equilibrium state are listed in the manner of "liquid / vapor".

area of Figure 2. The equivalent inner diameter, d_{eq}, is the diameter of a smooth tube that envelops an equal free flow volume. The surface enlargement, η_A, is the ratio of the actual heat transfer area to that of the equivalent smooth tube. Based on the actual heat transfer area, the heat flux, q, and the HTC, α, were defined as follows:

$$\alpha_{TS1} = q_{TS1} / \left(T_{r\,TS1} - T_{wi} \right), \quad q_{TS1} = Q_{H2O\,TS1} / \left(\pi d_{eq} \eta_A \Delta Z \right) \tag{8, 9}$$

A deviation within 1 kW m^{-2} of the targeted average heat flux was allowed to adjust for the test conditions, except for the dryout condition during the evaporation. The condensation and evaporation tests were carried out at the saturation temperatures, which are the average of the bubble and dew temperatures, 40 and 10 °C, respectively.

Table 2 compares the thermophysical properties between the test refrigerants at average saturation temperatures of 40 and 10 °C calculated with the REFPROP 9.1 (Lemmon et al., 2013). The mixing parameters for the combination of R32 and R1234ze(E) have been optimized by Akasaka et al. (2013) to fit the $P\rho T$ properties measured by Kobayashi et al. (2013). The following two indices, the bias, $\bar{\varepsilon}$, and the standard deviation, σ, will be used to compare the predicted values.

$$\bar{\varepsilon} = \frac{1}{n}\sum_{j=1}^{n} \varepsilon_j = \frac{1}{n}\sum_{j=1}^{n} \left[\left(\alpha_{cal,j} - \alpha_{exp,j} \right) / \alpha_{exp,j} \right] \text{ or } = \frac{1}{n}\sum_{j=1}^{n} \left[\left(\Delta P / \Delta Z_{cal,j} - \Delta P / \Delta Z_{exp,j} \right) / \left(\Delta P / \Delta Z_{exp,j} \right) \right] \tag{10}$$

$$\sigma = \sqrt{\frac{1}{n-1}\sum_{j=1}^{n} \left(\varepsilon_j - \bar{\varepsilon} \right)^2} \tag{11}$$

where n is the number of data points to be compared. The subscripts cal and exp indicate the prediction and the experiment.

3. RESULTS AND DISCUSSION

3.1 Condensation Heat Transfer

Figure 3 shows the variation in the condensation HTC as a function of the vapor quality at an average saturation temperature of 40 °C, a mass velocity 200 kg $m^{-2}s^{-1}$ and a heat flux of 10 kW m^{-2}. In Figures 3 (a), (b), and (c), the experimental HTC are plotted with symbols for the single components R32 and R1234ze(E) alone, the binary mixtures R32/R1234ze(E), and the ternary mixtures R744/R32/R1234ze(E), respectively. The horizontal and vertical bars appended to the symbols show the propagated measurement uncertainty of 95% coverage (Taylor, 1997) in the HTC and the vapor quality change in each subsection. The lines are the predicted HTC according to the correlation of Cavallini et al. (2009) with the correction method of Silver-Bell-Ghaly (1942, 1973) for non-azeotropic refrigerant mixtures. Tables 3 and 4 list the comparison results of HTC between the experiment and the correlations two indices, the bias $\bar{\varepsilon}$ and standard deviation σ.

As shown in Figure 3 (a), the HTC of R32 exceeds that of R1234ze(E), as predicted by the correlation. Other correlations listed in Table 3 also predict the same tendency. The higher liquid thermal conductivity and the larger latent heat of R32 increase the condensation HTC. The correlation proposed for the single components seems to properly include these effects to predict the condensation HTC. Nevertheless, the experimental HTC values deviate at vapor qualities beyond 0.7. According to Kedzierski and Goncalves (1999), this deviation is typically evident in the test section of a counter flow configuration, such as the one used in this study. They also tested the parallel flow and remarked that the drastic increases in HTC appear at higher vapor qualities and only with a counter flow configuration.

As shown in Figures 3 (b) and (c), the HTC values of binary and ternary mixtures are significantly lower than that of the single component. This difference typically is the result of the volatility difference. The less volatile components readily condense, while the more volatile components remain in the vapor phase. Therefore, the saturation temperature decreases as condensation proceeds. This phenomenon is dubbed temperature glide and requires

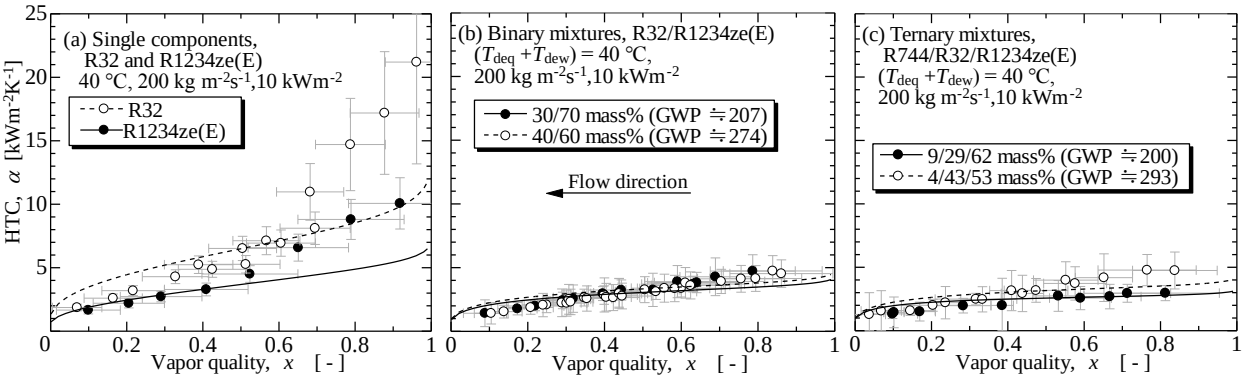

(a) single components (b) R32/R1234ze(E) (c) R744/R32/R1234ze(E)

Figure 3: Difference in condensation HTC between the single components and the mixtures (The lines are HTC predicted by correlations of Cavallini et al. (2009) with correction method of Silver-Bell-Ghaly (1942, 1973).

Table 3: Comparison of the condensation HTC between experiment and correlations for single components

	R32 n = 66		R1234ze(E) n = 50	
	$\bar{\varepsilon}$	σ	$\bar{\varepsilon}$	σ
Kedzierski and Goncalves (1999)	0.11	0.29	0.28	0.25
Chamra et al. (2005)	-0.01	0.45	-0.03	0.42
Yonemoto and Koyama (2007)	-0.09	0.32	0.05	0.25
Cavallini et al. (2009)	0.13	0.37	-0.01	0.28

Table 4: Comparison of the condensation HTC between experiment and correlations for zeotropic mixtures

R32/R1234ze(E) (n = 132)	$\bar{\varepsilon}$	σ
Cavallini et al. (2009) with Silver-Bell-Ghaly (1942, 1973)	0.00	0.35
Chamra and Mago (2006)	0.32	0.50
R744/R32/R1234ze(E) (n = 123)	$\bar{\varepsilon}$	σ
Cavallini et al. (2009) with Silver-Bell-Ghaly (1942, 1973)	0.01	0.33
Chamra and Mago (2006)	0.27	0.41

additional de-superheating to cool the vapor flow to the local saturation temperature downstream. In addition, a concentration boundary layer forms near the interface between the vapor and liquid, which is associated with the strong temperature distribution. The concentration boundary layer further disturbs smooth condensation, and the temperature distribution near the interface reduces the effective subcooling that is the driving force of condensation. Therefore, the HTC of zeotropic mixtures decreases from the ideal HTC calculated only with the thermophysical properties of normal condensing flow.

Silver (1942) shed light on the additionally required desuperheating to condense zeotropic mixtures, and Bell and Ghaly (1973) later proposed the correction method to include the sensible heat transfer in the total heat transfer of condensers. Smit et al. (2002) validated this correction method with their experimental data for R22/R142b. They demonstrated that the correction method works best with the correlation of Dabson and Chato (1998) proposed for normal condensation in horizontal smooth tubes. Therefore, the correlation of Cavallini et al. (2009), which shows good agreement for R32 and R1234ze(E), was selected for the microfin tubes. As shown in Figures 3 (b) and (c), the HTC of R744/R32/R1234ze(E) (9/29/62 mass%) is somewhat lower than those of the other binary and ternary mixtures. Among the thermophysical properties, only the temperature glide significantly differs, as listed in Table 2. The larger temperature glide of R744/R32/R1234ze(E) (9/29/62 mass%) requires more sensible heat transfer and reduces the effective subcooling more. As a result, the HTC of R744/R32/R1234ze(E) (9/29/62 mass%) is lower than that of the other ternary mixture.

Figures 4 (a) and (b) plot the HTC of ternary mixtures at mass velocities from 150 to 400 kg $m^{-2}s^{-1}$. The HTC values of these mixtures markedly increase as the mass velocity increases. The rate of this increase in the HTC is more significant than that of the single component. At mass velocities of 400 kg $m^{-2}s^{-1}$ and beyond, the HTC seems to revert to values similar to that of the single components. The predictions obtained using the Silver-Bell-Ghaly correction method apparently agree well with the experimental data at a mass velocity of 200 kg $m^{-2}s^{-1}$, as shown in Figure 3; however, the experimental HTC deviates from the predicted HTC, especially at mass velocities above 300 kg $m^{-2}s^{-1}$.

Figure 4 (c) plots the variation in HTC of R744/R32/R1234ze(E) (9/29/62 mass%) as the function of the mass velocity. The symbols are the experimental HTC extracted from the data over vapor quality range from 0.4 to 0.6. The solid line is the predicted HTC calculated using the correlation of Cavallini et al. (2009) associated with Silver-Bell-Ghaly (1942, 1973). The dashed line is the ideal HTC that is calculated using the correlation of Cavallini et al. (2009) alone while simply considering the effect of thermophysical properties in "normal" condensation. The experimental HTC of the ternary mixture approaches that of the ideal HTC as the mass velocity increases. This finding suggests that increasing the mass velocity mitigates the mass transfer resistance caused by the volatility difference. Smit and Meyer (2002) experimentally confirmed a similar effect. The mass fraction of refrigerant mixture R22/R142b influences the average HTC at vapor qualities ranging from 0.1 to 0.85 and mass velocities between 40 to 350 kg $m^{-2}s^{-1}$; on the contrary, it does not influence the HTC at mass velocities beyond 350 kg $m^{-2}s^{-1}$. Although the critical mass velocity at which the influence of the mass transfer resistance vanishes is different, these two results are qualitatively identical. The concentration boundary layer is most likely thinned and partly broken at higher refrigerant flow speeds, and the critical mass velocity depends on the magnitude of the volatility difference.

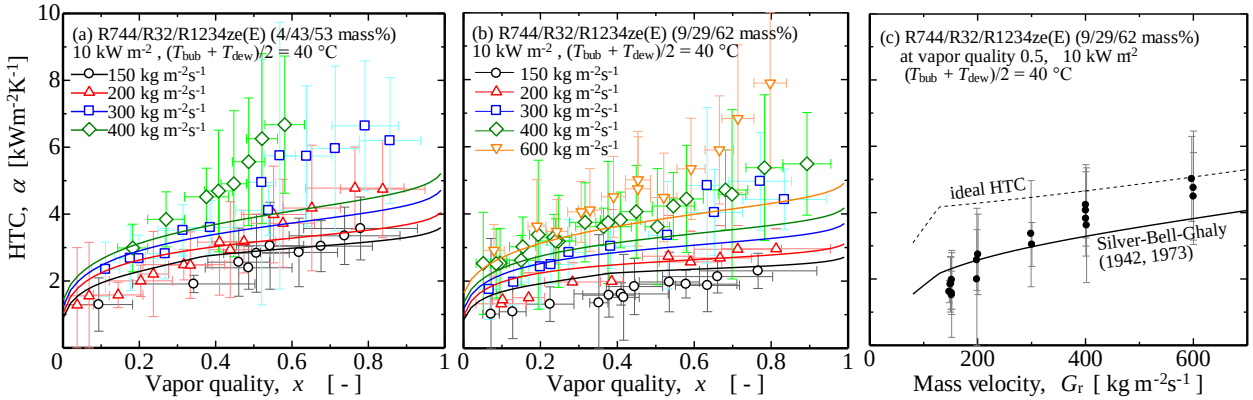

(a) 4/43/53 mass% (b) 9/29/62 mass% (c) comparison with ideal HTC

Figure 4: Mitigation of mass transfer resistance by increasing mass velocity in condensation HTC

3.2 Evaporation Heat Transfer

Figures 5 (a), (b), and (c) plot the evaporation HTC of the single components R32 and R1234ze(E) alone, the binary mixtures R32/R1234ze(E), and the ternary mixtures R744/R32/R1234ze(E), respectively, at an average saturation temperature of 10 °C, a mass velocity 200 kg $m^{-2}s^{-1}$, and a heat flux of 10 kW m^{-2}. The lines are the predicted HTC calculated by the correlation of Mori et al. (2002) for single components, and of Cavallini et al. (1998) for the binary and ternary mixtures. The onset and completion dryout qualities and post-dryout HTC are predicted by the correlation of Yoshida et al. (2000) and Mori et al. (2000).

Compared in Figure 5 (a), the HTC of R32 markedly exceeds that of R1234ze(E). This finding is primarily attributed to the higher liquid thermal conductivity and the larger latent heat of R32, as listed in Table 2. The surface tension of R32 is smaller than that of R1234ze(E) at a given saturation temperature, and this difference reduces the bubble departure diameter and increases the bubble departure frequency. Thus, this effect enhances the nucleate boiling contribution at lower vapor qualities of approximately less than 0.4. Table 5 lists the deviation of the predicted HTC from the experimental HTC, i.e. $\bar{\varepsilon}$ and σ. These deviations are acceptably small, except for that of the correlation proposed by Chamra and Mago (2007), and these correlations accurately predict the evaporation HTC for both the single components R1234ze(E) and R32.

As plotted in Figures 5 (b) and (c), the evaporation HTC values of the binary and ternary mixtures are drastically lower than those of the single components. This behavior is typical of zeotropic mixtures. The evaporation process enriches the liquid phase in the less volatile components due to this volatility difference, while the vapor phase becomes richer in the more volatile components. Thus, a concentration boundary forms over the liquid-vapor interface and in the superheated sublayer of the nucleate boiling site adjacent to the tube wall. Therefore, the saturation temperature is locally increased in the rich concentration boundary layer of the less volatile component. This increase requires more heating to yield nucleate boiling on the tube wall and to evaporate the liquid-vapor interface. Moreover, additional heat is required to heat the vapor flow to the local saturation temperature because of

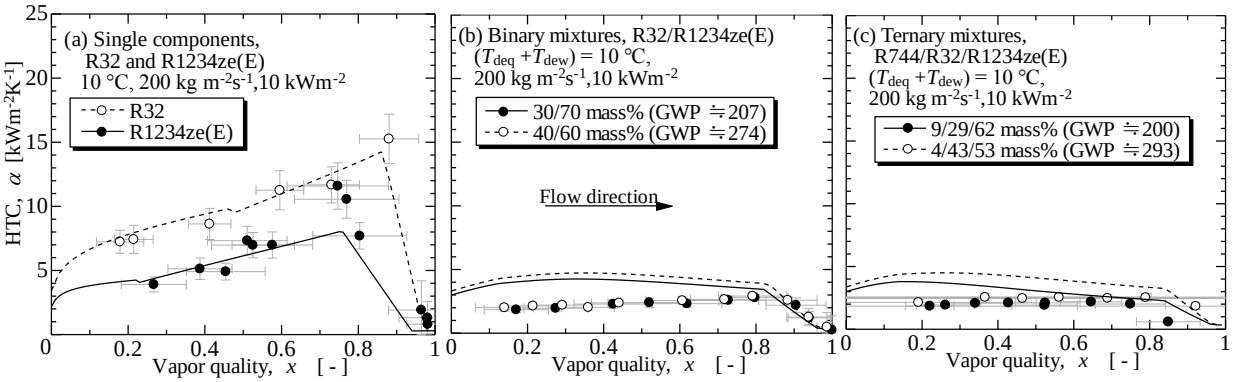

(a) single components (b) R32/R1234ze(E) (c) R744/R32/R1234ze(E)

Figure 5: Difference in evaporation HTC between the single components and the mixtures. (The lines are HTC predicted by correlations of Mori (2002) for single components and Cavallini et al. (1998) for mixtures.)

Table 5: Comparison of the evaporation HTC between experiment and correlations for the single components

	R32 n = 90		R1234ze(E) n = 44	
	$\bar{\varepsilon}$	σ	$\bar{\varepsilon}$	σ
Momoki et al. (1995)	-0.04	0.23	0.11	0.36
Thome et al. (1997)	0.02	0.18	0.18	0.46
Mori et al. (2002)	-0.01	0.17	0.13	0.45
Yun et al. (2002)	-0.04	0.31	-0.41	0.33
Chamra and Mago (2007)	1.01	0.51	0.92	0.92

Table 6: Comparison of the condensation HTC between experiment and correlations for the zeotropic mixtures

R32/R1234ze(E) (n =189)	$\bar{\varepsilon}$	σ
Murata (1996)	2.64	4.70
Cavallini et al. (1998)	0.54	0.42
Chamra and Mago (2007)	-0.14	0.33
R744/R32/R1234ze(E) (n =128)	$\bar{\varepsilon}$	σ
Cavallini et al. (2007)	0.59	0.34
Chamra et al. (2006)	-0.20	0.21

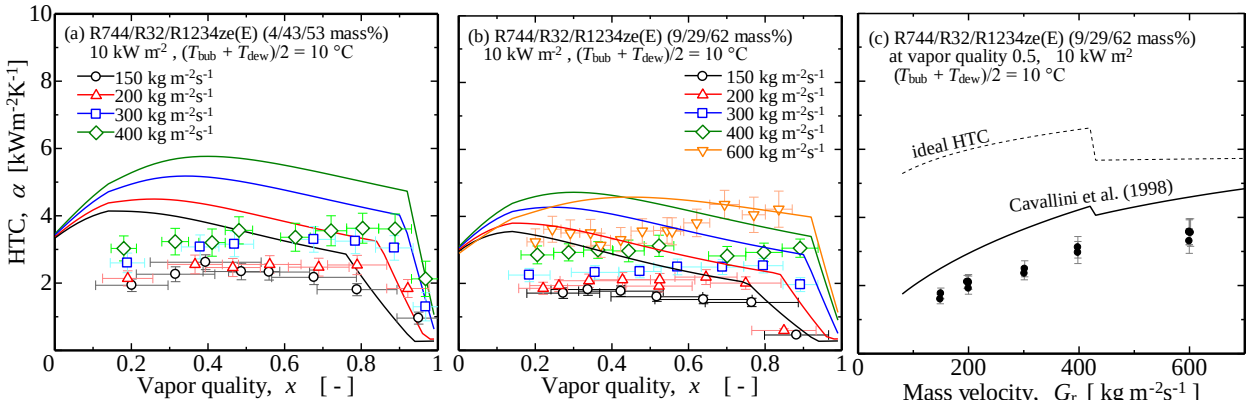

(a) 4/43/53 mass% (b) 9/29/62 mass% (c) comparison with ideal HTC

Figure 6: Effect of mass velocity on mass transfer resistance in evaporation HTC

the temperature glide, as mentioned by Butterworth (1981) and Stephan (1992). Therefore, the heat transfer degradation is distinct in the evaporation HTC of the zeotropic mixtures for the entire range of vapor quality. Table 6 lists the deviation between the predicted HTC and the experimental HTC. Despite the complicating mechanism of the volatility difference, the selected correlations satisfactorily agree with the experimental HTC, except for the correlation proposed by Murata (1996) for binary mixtures. A comparison of the HTC between mixtures shows that the HTC of R744/R32/R1234ze(E) (9/29/62 mass%), which showed the largest temperature glide, is slightly lower and begins dryout at a slightly lower vapor quality than the other mixtures. The correlation proposed by Cavallini et al. (1998) qualitatively predicts this difference, as shown in Figures 5 (b) and (c).

Figures 6 (a) and (b) plot the evaporation HTC of R744/R32/R1234ze(E) (4/43/53 mass%) and (9/29/62 mass%), respectively, at mass velocities from 150 to 600 kg $m^{-2}s^{-1}$. The lines are the predicted HTC calculated using the correlation of Cavallini et al. (1998) as well as that of Yoshida et al. (2000) and Mori et al. (2000) for the dryout region. The correlation of Cavallini et al. (1998) unfortunately overestimates the HTC at lower vapor qualities. If the suppression of nucleate boiling by the volatility difference were more accurately predicted, the correlation would show excellent agreement with the present experimental HTC. The experimental data showed an obvious positive correlation with the mass velocity, and the correlation qualitatively predicts this effect.

Figure 6 (c) shows the variation in the evaporation HTC of R744/R32/R1234ze(E) (9/29/62 mass%) as a function of the mass velocity. The symbols are the experimental HTC extracted from the database for vapor qualities ranging from 0.4 to 0.6. The solid line shows the predicted HTC of zeotropic mixtures calculated using the correlation of Cavallini et al. (1998). The dashed line shows the ideal HTC calculated using the correlation of Cavallini et al. (1998), which only considers the effect of the thermophysical properties and was proposed for single components. The experimental HTC approaches the ideal HTC. Increasing the mass velocity apparently mitigates the influence of the mass transfer resistance, and the predicted HTC exhibits this effect very well. In contrast to the condensation, the HTC of the mixture remains lower than that of the ideal HTC. The influence of the mass transfer resistance seems to be more severe in evaporation heat transfer.

3.3 Pressure Gradient

Figures 7 (a) and (b) plot the pressure gradient of the ternary mixtures during condensation and evaporation, respectively, at mass velocities of 150 and 400 kg $m^{-2}s^{-1}$. The lines are the pressure gradient predicted by the correlation of Yonemoto-Koyama (2007) and Kubota et al. (2001) for condensation and evaporation, respectively. Even though these correlations were proposed for single components and not zeotropic mixtures, they accurately predict the pressure gradient of the mixtures. As listed in Table 7, other correlations for the single components also agreed well with the experimental HTC. The influence of the volatility difference on the pressure gradient is seemingly negligible. Therefore, the pressure gradients of these two mixtures of similar thermophysical properties are comparable, despite the difference in the temperature glide. The pressure gradient during the evaporation is considerably larger than that of the condensation because the vapor density is smaller at lower reduced pressures, i.e. lower saturation temperatures.

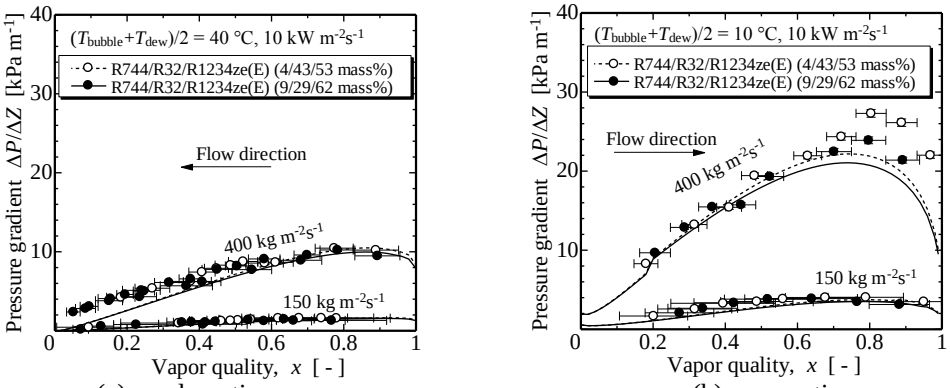

(a) condensation (b) evaporation

Figure 7: Pressure gradient of the ternary mixtures. (The lines are the prediction of Yonemoto-Koyama (2007) and Kubota et al. (2001) for condensation and evaporation respectively.)

Table 7: Comparison of the pressure gradient between experiment and correlations for zeotropic mixtures

Condensation			Evaporation		
R744/R32/R1234ze(E) (n =128)	$\bar{\varepsilon}$	σ	R744/R32/R1234ze(E) (n =156)	$\bar{\varepsilon}$	σ
Cavallini et al. (1997)	0.08	0.18	Goto et al. (2001, 2007)	-0.38	0.14
Goto et al. (2001, 2007)	-0.42	0.11	Newell and Shah (2001)	-0.02	0.25
Yonemoto and Koyama (2007)	-0.24	0.22	Kubota et al. (2001)	-0.10	0.13
Newell and Shah (2001)	-0.35	0.21	Filho et al. (2004)	0.50	0.19

4. CONCLUSIONS

The heat transfer coefficient and pressure gradient of the binary mixtures R32/R1234ze(E) and the ternary mixtures R744/R32/R1234ze(E) with a GWP of approximately 200 and 300 in horizontal microfin tubes have been experimentally investigated in this study. The condensation HTC of R32 alone is somewhat higher than that of R1234ze(E) due to superior thermophysical properties, as predicted by the correlations. However, the HTC values of the binary and ternary mixtures are drastically lower those that of the single components. The HTC severely decreased due to the mass transfer resistance. This severe influence of the mass transfer resistance was quantified: the influence is obviously mitigated by increasing the mass velocity. At mass velocities exceeding 400 kg m^{-2}s^{-1}, the HTC of the mixture approaches that of the single component. The correction method proposed by Silver-Bell-Ghaly (1942, 1973) predicts the influence of the mass transfer resistance in general; however, this correction underestimates the HTC at higher velocities, where the mass transfer resistance is fully mitigated. Similar to the condensation HTC, the evaporation HTC of R32 alone is higher than that of the R1234ze(E) alone. The evaporation HTC values of the binary and ternary mixtures were also drastically lower those that of the single components due to the mass transfer resistance caused by the volatility difference. The mass transfer resistance appears to suppress the nucleate boiling contribution and the forced convective contribution. Therefore, the decrease in the HTC is more severe for the evaporation than the condensation. Despite the complicating mechanism of the mass transfer resistance, the experimental HTC and predicted HTC by Cavallini et al. (1998) showed satisfactory agreement. The correlation proposed for single components for the condensation and the evaporation accurately predicted the pressure gradients of the mixtures. The influence of the volatility difference on the pressure gradient is negligible.

NOMENCLATURE

D_o	outer diameter	(m)	**Subscripts**
P	pressure	(Pa)	bottom bottom

Q	heat transfer rate	(W)	cal	calculation
T	temperature	(°C)	exp	experiment
X	mass fraction	(-)	H2O	water
Z	tube length	(m)	i	inlet
d_{eq}	equivalent inner diameter	(m)	left	left
h	enthalpy	(J kg^{-1})	o	outlet
n	number of data points	(-)	R32	R32
q	heat flux	(W m^{-2})	R744	R744
x	vapor quality	(-)	right	right
α	heat transfer coefficient	(W $m^{-2}K^{-1}$)	TS	test section
ε	bias	(-)	top	top
η_A	surface enlargement	(-)	tube	tube
λ	thermal conductivity	(W $m^{-1}K^{-1}$)	wi	inner wall
σ	standard deviation	(-)	wo	outer wall

REFERENCES

Akasaka, R., 2013, Thermodynamic Property Models for the Difluoromethane (R-32) + Trans-1,3,3,3- tetrafluoro propene (R-1234ze(E)) and Difluoromethane + 2,3,3,3- Tetrafluoropropene (R-1234yf) Mixtures, *Fluid Phase Equilibria*, vol. 358: p. 98-104.

Bell, K.J., Ghaly, M.A., 1973, An approximate generalized design method for multicomponent/partial condenser *AIChE Symp. Ser*., vol. 69: p.72-79.

Butterworth, D., 1981, *Unsolved problems in heat exchanger design, Heat Exchangers*: Thermal-Hydraulic Fundamentals and Design. Edited by Kakac, S., Bergles, A. E., Mayinger. F., Hemisphere, Washington, p. 1093-1096.

Cavallini, A., DelCol, D., Mancin, S., Rossetto, L., 2009, Condensation of pure and near-azeotropic refrigerants in microfin tubes: A new computational procedure, *Int. J. Refrig*., vol. 32: p. 162–174.

Cavallini, A., DelCol, D., Doretti, L., Longo, G.A., Rossetto, L.,1997, Pressure drop during condensation and vaporisation of refrigerants inside enhanced tubes, *Int. J. Heat & Technology*, vol. 15: p.3-10.

Cavalllini, A., DelCol, D., Longo, G.A., Rosset, L., 1998, Refrigerant vaporization inside enhanced tubes, *Proc. Heat Transfer in Condensation and Evaporation*, Eurotherm seminar, Grenoble, France: p. 222-231.

Chamra, L.M., Mago, P.J., Tan, M.O., Kung, C.C., 2005, Modeling of condensation heat transfer of pure refrigerants in micro-fin tubes, *Int. J. Heat and Mass Transfer.* vol. 48: p. 1293-1302.

Chamra, L.M., Mago, P.J., 2006, Modeling of condensation heat transfer of refrigerant mixture in micro-fin tubes, *Int. J. Heat and Mass Transfer*., vol. 49: p. 1915-1921.

Chamra, L.M., Mago, P.J., 2007, Modelling of evaporation heat transfer of pure refrigerants and refrigerant mixtures in microfin tubes. *Proc. IMechE., 221, Part C: J. Mechanical Engineering Science*: p. 443-454.

Dobson, M.K., and Chato, J.C., 1998, Condensation in Smooth Horizontal Tubes, *J. Heat Transfer, Trans. ASME*, vol. 120: p. 193-213

Filho, E.P.B., Jabardo, J.M.S., Barbieri, P.E.L., 2004, Convective boiling pressure drop of refrigerant R-134a in horizontal smooth and microfin tubes, *Int. J. Refrig.*, vol. 27: p. 895-903.

Fukuda, S., Kondou, C., Takata, N., Koyama, S., 2014, Cycle performance of low GWP refrigerant mixtures R-32/1234ze(E) and R-744/32/1234ze(E), *Proc. 7th Asian Conference on Refrigeration and Air Conditioning*, paper no. ACRA2014-421.

Goto, M., Inoue, N., Ishiwatari, N., 2001, Condensation and evaporation heat transfer of R410A inside internally grooved horizontal tubes, *Int. J. Refrig*., vol. 24: p. 628-638.

Goto, M., Inoue, N., Ishiwatari, N., 2007, Answer to comments by M.M. Awad, *Int. J. Refrig*., vol. 30: p. 1467.

Jakobs, R., Kruse, H., 1978, The use of non-azeotropic refrigerant mixture in heat pumps for energy saving, *Proc. IIR Commissions B2*: p. 207-218.

Jung, D., Radermacher, R., 1993, Prediction of evaporation heat transfer coefficient and pressure drop of refrigerant mixtures in horizontal tubes, *Int. J. Refrig*., vol. 16: p. 201-209.

Kedzierski, M.A., Goncalves, J.M., 1999, Horizontal convective condensation of alternative refrigerants within a micro-fin tube, *Enhanced Heat Transfer*, vol. 6: p. 161-178.

Kobayashi, K., Tanaka, K., Higashi, Y., 2011, PρTχ Property Measurements of Binary HFO-1234ze(E)+HFC-32 Refrigerant Mixtures, *Trans. JSRAE*, vol. 28, no. 4: p. 415-426 (in Japanese).

Koyama, S., Higashi, T., Miyara, A., Akasaka, R., 2013, Research and development of low-GWP refrigerants suitable for heat pump systems. In: *JSRAE Risk Assessment of Mildly Flammable Refrigerants-2012 Progress Report*, JSRAE: p. 29-34.

Kubota, A., Uchida, M., Shikazono, N., 2001, Predicting equations for evaporation pressure drop inside horizontal smooth and grooved tubes, *Trans. JSRAE*, vol. 18 no. 4: p. 393-401 (in Japanese).

Lemmon, E.W., Huber, M.L., McLinden, M.O., 2013, Reference Fluid Thermodynamic and Transport Properties - REFPROP Ver. 9.1, National Institute of Standards and Technology, Boulder, CO, USA.

McLinden, M.O. and Radermacher, R., 1987, Mothod for comparing the performance of pure and mixed refrigerants in the vapour compression cycle, *Int. J. Refrig*., vol. 10: p. 318-325

Momoki, S., Yu, J., Koyama, S., Fujii, T., Honda, H., 1995, A correlation for forced convective boiling heat transfer of refrigerants in a microfin tube, *Trans. JAR*, vol. 12, no. 2, p. 177-184 (in Japanese).

Mori, H., Yoshida, S., Kakimoto, Y., Ohishi, K., and Fukuda, K., 2000, Post-dryout heat transfer to a refrigerant flowing in horizontal evaporator tubes, *Trans. JSRAE*, vol. 4: p. 521-528 (in Japanese).

Mori, H., Yoshida, S., Koyama, S., Miyara, A., Momoki, S., 2002, Prediction of heat transfer coefficients for refrigerants flowing in horizontal spirally grooved evaporator tubes, *Proc. 14th JSRAE Annual Conf.*: p. 97-100 (in Japanese).

Murata, K., 1996, Correlation for forced convective boiling heat transfer of binary refrigerant mixtures -2nd report: a spirally grooved tube, *Trans. JSME* (B), vol. 62, no. 599: p. 2723-2728 (in Japanese).

Newell, T.A., Shah, R.K., 2001, An assessment of refrigerant heat transfer, pressure drop, and void fraction effects in microfin tubes, *HVAC&R Research*, vol. 7, no. 2: p. 125-153.

Niederküger, M., Steiner, D., 1994, Flow boiling heat transfer to saturated pure components and non-azeotropic mixtures in a horizontal tube, *Chem. Eng. Prog*., vol. 33: p. 261-275.

Silver, L., 1942, Gas cooling with aqueous condensation, *Trans. Inst. Chem. Eng*., vol. 20, no. 14: p. 30-42.

Smit, F.J., Thome, J.R., Meyer, J.P., 2002, Heat transfer coefficients during condensation of the zeotropic refrigerant mixture HCFC-22/HCFC142b, *J. Heat Transfer, Trans. ASME*, vol. 124: p. 1137-1146.

Smit, F.J., Meyer, J.P., 2002, Condensation heat transfer coefficient of the zeotropic refrigerant mixture R-22/R142b in smooth horizontal tubes. *Int. J. Thermal Science*, vol. 41: p. 625-630.

Stephan, K., 1992, *Heat transfer in condensation and boiling*, Translated by Green, C.V., Springer-Verlag, Berlin, Heidelberg, p. 286-291.

Taylor, J.T., 1997, *An introduction to error analysis*, 2nd ed., University science book.

Thome, J.R., Kattan, N., Favrat, D., 1997, Evaporation in microfin tubes: a generalized prediction model, *Proc. Convective Flow and Pool Boiling Conf.*, Kloster Irsee, Germany, Paper VII-4.

Yonemoto R., Koyama S., 2007, Experimental study on condensation of pure refrigerants in horizontal micro-fin tubes: proposal of correlations for heat transfer coefficient and frictional pressure drop, *Trans. JSRAE*, vol. 24**,** no. 2: p. 139-148, (in Japanese).

Yoshida, S., Mori, H., Kakimoto, Y., and Ohishi, K., 2000, Dryout quality for refrigerants flowing in horizontal evaporator tubes, *Trans. JSRAE*, vol. 4, p. 511-520 (in Japanese)

Yun, R., Kim, Y., Seo, K., Kim, H.Y., 2002, A generalized correlation for evaporation heat transfer of refrigerants in micro-fin tube, *Int. J. Heat Mass Transfer*, vol. 45: p. 2003-2010.

ACKNOWLEDGMENTS

The work presented here was financially supported by the New Energy and Industrial Technology Development Organization (NEDO). The test tubes were kindly provided by Kobelco and Materials Copper Tube, Ltd.